View metadata, citation and similar papers at core.ac.uk
brought to you by CORE
provided by eprints@NML

ELSEVIER
Available online at www.sciencedirect.com
SCIENCE DIRECT®
Materials Letters 60 (2006) 1990–1995
materials letters
www.elsevier.com/locate/matlet

Pulsed electrodeposition of nanocrystalline Cu–Ni alloy films and evaluation of their characteristic properties

I. Baskaran [a], T.S.N. Sankara Narayanan [b,*], A. Stephen [a]

[a] *Materials Science Centre, Department of Nuclear Physics, University of Madras, Guindy Campus, Chennai-600 025, India*
[b] *National Metallurgical Laboratory, Madras Centre, CSIR Complex, Taramani, Chennai-600 113, India*

Received 12 February 2005; accepted 19 December 2005
Available online 10 January 2006

Abstract

The preparation of nanocrystalline Cu–Ni alloy films by pulsed electrodeposition process and their structural, morphology, thermal characteristics and magnetic properties are addressed. The study reveals that the film composition, lattice constant and magnetic properties of the films could be controlled by the applied current density and duty cycle. Energy dispersive X-ray analysis (EDX) confirms that the Cu–Ni alloy film has a stoichiometry of $Cu_{0.98}Ni_{0.02}$, $Cu_{0.95}Ni_{0.05}$, $Cu_{0.89}Ni_{0.11}$, $Cu_{0.77}Ni_{0.23}$, $Cu_{0.56}Ni_{0.44}$ and $Cu_{0.38}Ni_{0.62}$ that are obtained at 2.5, 5, 7.5, 10, 15 and 20 A/dm^2, respectively. The X-ray diffraction (XRD) measurements confirm that all the six Cu–Ni alloy films of the present study possess the f.c.c. structure. The lattice constant is found to decrease with increase in nickel content of the Cu–Ni alloy. The crystallite size lies in the range of 15 to 46 nm for as-plated alloys and increases from 20 to 114 nm, following vacuum annealing at 400 °C for 1 h. The differential scanning calorimetry (DSC) trace indicates a broad exothermic peak characteristic of nanocrystalline materials. The vibrating sample magnetometer (VSM) study reveals that, among the six types of Cu–Ni alloy films, the films obtained at 2.5 and 5.0 A/dm^2 are diamagnetic; the one obtained at 7.5 A/dm^2 is weakly ferromagnetic, whereas those obtained at 10, 15 and 20 A/dm^2 are ferromagnetic. The saturation magnetization increases with increase in nickel content of the Cu–Ni alloy film.
© 2005 Elsevier B.V. All rights reserved.

Keywords: Pulse plating; Electrodeposition; Nanocrystalline; Cu-Ni alloy films; Magnetic properties

1. Introduction

The discovery of novel nanoscale phenomena and their potential application in a variety of areas such as micro- and nano-electronics has led to a rapid increase in research on functional properties of nanostructures [1,2]. In most cases, these materials are fabricated by vacuum deposition, sputtering, sol–gel, spray pyrolysis, etc. All these methods require a high degree of process control, which could be accomplished only with the use of expensive equipment and involve a huge wastage of materials. Preparation of nanostructured materials by electrodeposition technique has received much interest in recent years and they have been utilized for a variety of applications such as magnetic materials, noble metal catalysts, etc. [3–5]. Electrodeposition is a very simple and cost-effective fabrication process. It has the advantage of preparing films over a large surface area in a relatively shorter period without sacrificing the materials purity. Copper plating is used in the semiconductor

Table 1
Bath composition and operating conditions employed for preparing nanocrystalline Cu–Ni alloy by pulsed electrodeposition process

Bath composition	
Nickel sulphate hexahydrate	0.02 M
Copper sulphate pentahydrate	0.002 M
Trisodium citrate	0.2 M
Operating conditions	
pH	5.0
Temperature	55 ± 1 °C
Agitation	300 rpm—using magnetic stirrer
Current density	2.5, 5, 7.5, 10, 15 and 20 A/dm^2
T_{ON}	1 ms
T_{OFF}	9 ms
Frequency (duty cycle) [a]	100 Hz (10%)

[a] Duty cycle (%) = $T_{on}/(T_{off}+T_{on})\times 100$.

* Corresponding author.
E-mail addresses: tsnsn@rediffmail.com (T.S.N. Sankara Narayanan), Stephen_arum@hotmail.com (A. Stephen).

0167-577X/$ - see front matter © 2005 Elsevier B.V. All rights reserved.
doi:10.1016/j.matlet.2005.12.065

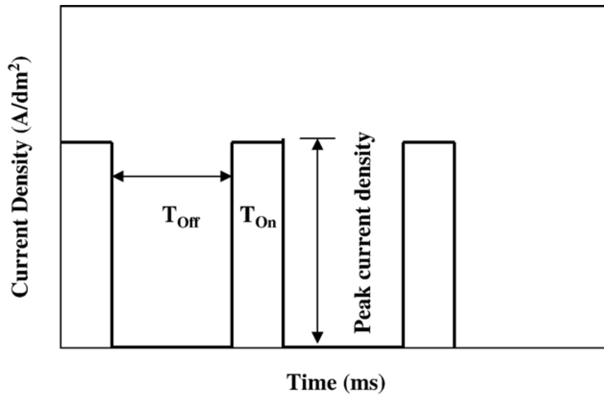

Fig. 1. The current wave form employed for the pulsed current electrodeposition of Cu–Ni alloy films.

industry for fabrication of metallic interconnects [6]. Pure Ni, Cu–Ni alloy and pure Cu thin films are used in the microelectronics packaging industry and mobile electronics, such as notebook computers, cellular phones, chips and personal digital assistants [7]. The binary Cu–Ni alloys are widely used in mining and metallurgical works, in chemical industry owing to their high corrosion resistance and mechanical properties. Besides, the Cu–Ni alloys have received much attention for their magnetic and thermophysical properties and are also used for decorative purposes [8–10].

Electrodeposition is one of the most commonly employed techniques for preparing Cu–Ni alloys [11,12]. The standard reduction potential for copper and nickel are +0.35 and −0.25 V, respectively, which are far apart from each other. Hence, under direct current (DC) plating conditions, only above a critical current density, the Cu–Ni alloy could be deposited. Preparing nanosized Cu–Ni alloy deposits require the application of much higher current densities, which normally results in films with cracks and pores. In contrast to DC plating, pulsed electrodeposition (PED) offers unique advantages such as deposition of uniform and crack free coating with desirable characteristics [13–18]. In this perspective, the present work aims to study the formation of Cu–Ni alloy films by PED technique and to evaluate their characteristic properties.

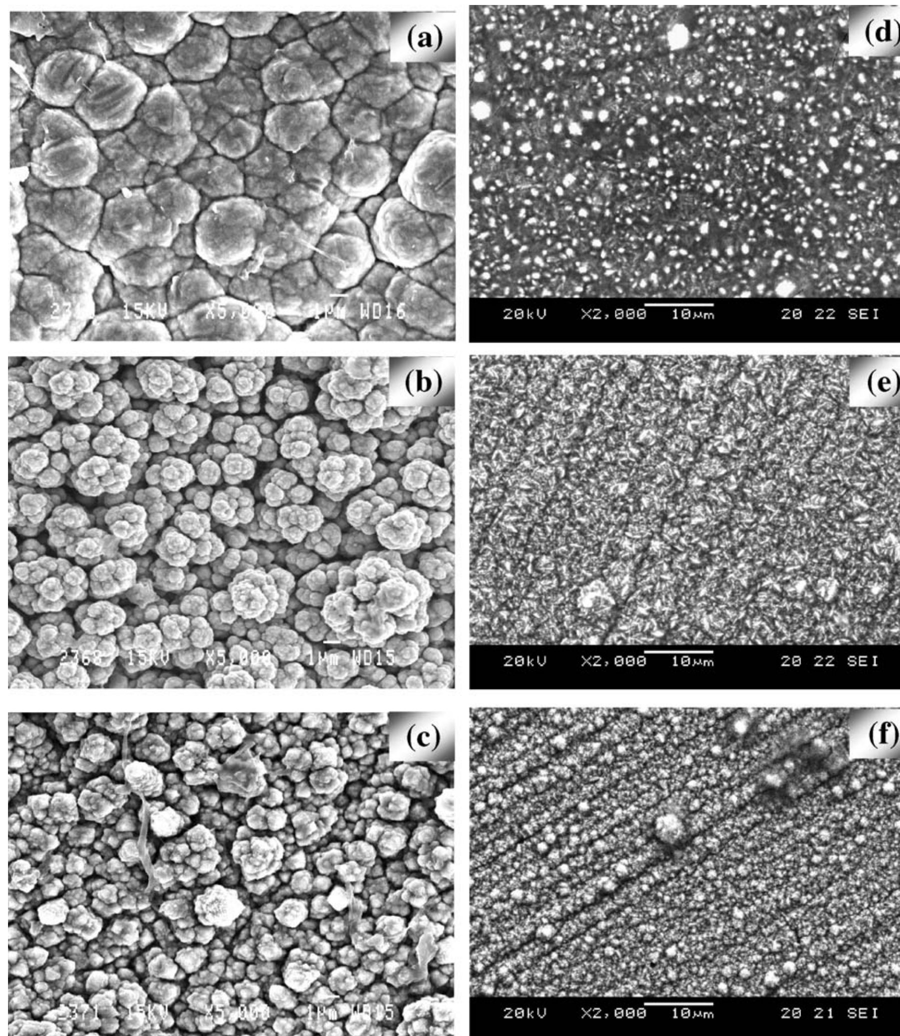

Fig. 2. Scanning electron micrographs of the Cu–Ni alloy films obtained by PED at different current densities (a) 2.5 A/dm^2, (b) 5.0 A/dm^2, (c) 7.5 A/dm^2, (d) 10 A/dm^2, (e) 15 A/dm^2 and (f) 20 A/dm^2.

2. Experimental details

Cu–Ni alloy films were deposited on electrolytic grade copper substrates (40 mm × 30 mm × 1 mm). The copper substrate was mechanically polished using SiC abrasive paper and subsequently treated for a few seconds in dilute HNO_3 (v/v 1:1) in order to remove the impurities. The substrate surface was then chemically treated for a few seconds in a dilute HCl (v/v 1:3). PED of the Cu–Ni alloy films was carried out using a plating bath that contains nickel sulphate hexahydrate as the source of nickel, copper sulphate pentahydrate as the source of copper and sodium citrate as the complexing agent. Sodium citrate was chosen as the complexing agent due to its ability to improve the deposition efficiency, to obtain stress-free deposits even at very high current densities and its relatively less toxic nature. Citrate-based plating bath has also been used earlier by Priscott [12], Vu Quang et al. [19] and Ying [20] to prepare Cu–Ni alloy films. All the reagents used in this study were of Analar grade and were used as such without further purification. Double-distilled water was used to prepare the plating solution. Since the standard reduction potential of copper and nickel are far apart from each other, the concentration of copper ions in the plating bath was kept relatively lower than that of nickel. The bath composition and operating conditions of the plating bath employed for preparing Cu–Ni alloy films are given in Table 1.

PED was performed in an electrolytic cell containing 250 ml of the plating solution. Only one side of the copper substrate was employed for deposition of the Cu–Ni alloy films, whereas the other side of the substrate was masked using a non-conducting resin. A rectangular graphite plate, similar in size as that of the copper cathode, was employed as the anode. The graphite anode was covered with a muslin bag to avoid contamination of the bath with the graphite particles. During plating, the plating bath was agitated using a magnetic stirrer (300 rpm) to ensure a uniform supply of the metal ions towards the cathode–solution interface. The temperature of the bath was maintained at 55 ± 1 °C using a constant temperature oil bath. The PED Cu–Ni films were prepared at different applied current densities in the range of 2.5–20 A/dm^2. The current waveform employed for the PED is depicted in Fig. 1. During plating, the current was applied for 1 ms (T_{ON}—pulse-on-period) and cut-off for 9 ms (T_{OFF}—pulse-off-period). The duty cycle, defined as $T_{ON}/(T_{ON}+T_{OFF})$, was 10% and the frequency was 100 Hz. After deposition, the Cu–Ni alloy films were rinsed with deionized water and dried using hot air.

The structural characteristics of the Cu–Ni alloy films, both as-plated and vacuum annealed at 400 °C for 1 h, were investigated by X-ray diffraction measurement (XRD) using a Cu Kα_1 radiation (λ = 1.5406 Å) (Rich Siefert-Model 3000). The surface morphology of the Cu–Ni alloy films was assessed using a scanning electron microscope (SEM). The chemical composition of the Cu–Ni alloy films was determined by the energy dispersive X-ray analysis (EDX). The phase transformation behaviour of the Cu–Ni alloy films was studied using a Perkin Elmer differential scanning calorimetry (DSC) (Model-DSC-7) in an argon flux (10 cc/min) at a heating rate of 10 °C/min. The magnetic properties of the Cu–Ni alloy films were determined using a vibrating sample magnetometer (VSM) (Model: EG&G-4500).

3. Results and discussion

The Cu–Ni alloy films are obtained at six different current densities, viz., 2.5, 5, 7.5, 10, 15 and 20 A/dm^2, all at a frequency of 100 Hz. The Cu–Ni alloy films obtained at 2.5 and 5 A/dm^2 are rich in copper colour; the films obtained at 7.5 and 10 A/dm^2 possess a slight metallic nickel luster, whereas the films obtained at 15 and 20 A/dm^2 are rich in nickel colour. This visual observation suggests that the Cu–Ni alloy films are predominantly copper at low current densities and consist of both copper and nickel at moderate current densities and predominantly nickel at high current densities. The dependence of the composition of the Cu–Ni alloy films on the applied potential has also been reported earlier by Bennett et al. [21,22]. They have confirmed that, at low applied potentials, only the more noble copper is deposited, while, when the potential is set at a value corresponding to nickel, both metals will be reduced at rates limited by their relative concentrations, resulting in a structure of unalloyed copper alternating with nickel having low copper content. Since the Cu–Ni alloy films of the present study are prepared by PED process, it is expected that, besides the applied potential, the pulse duration would also influence the Cu–Ni alloy formation. It is presumed that, during the 'ON' time, the deposit might be an alloy of Cu–Ni, whereas, during the relaxation ('OFF') time, the alloy film might be mainly copper. Ghosh et al. [23] have also confirmed such an occurrence in PED Cu–Ni alloy films.

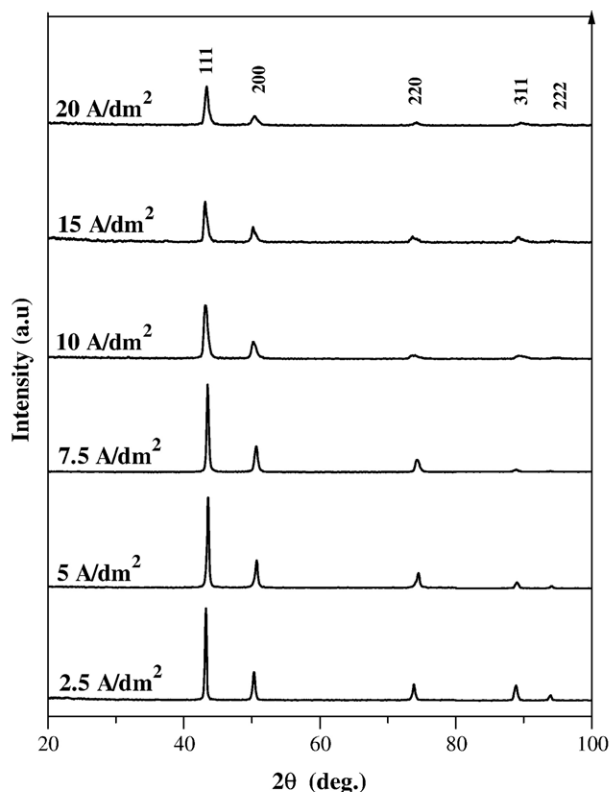

Fig. 3. X-ray diffraction pattern of the Cu–Ni alloy films obtained by PED at 2.5, 5, 7.5, 10, 15 and 20 A/dm^2 in their as-deposited condition.

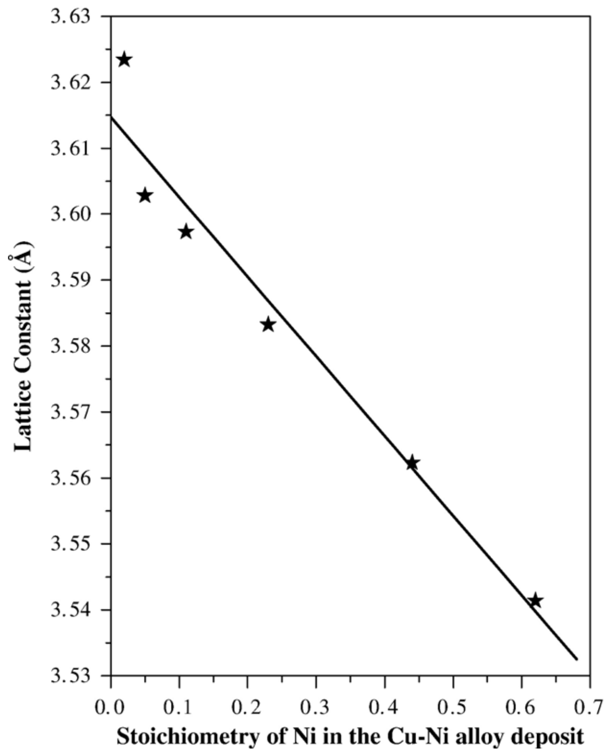

Fig. 4. Plot of the lattice constant of the Cu–Ni alloy film as a function of film composition.

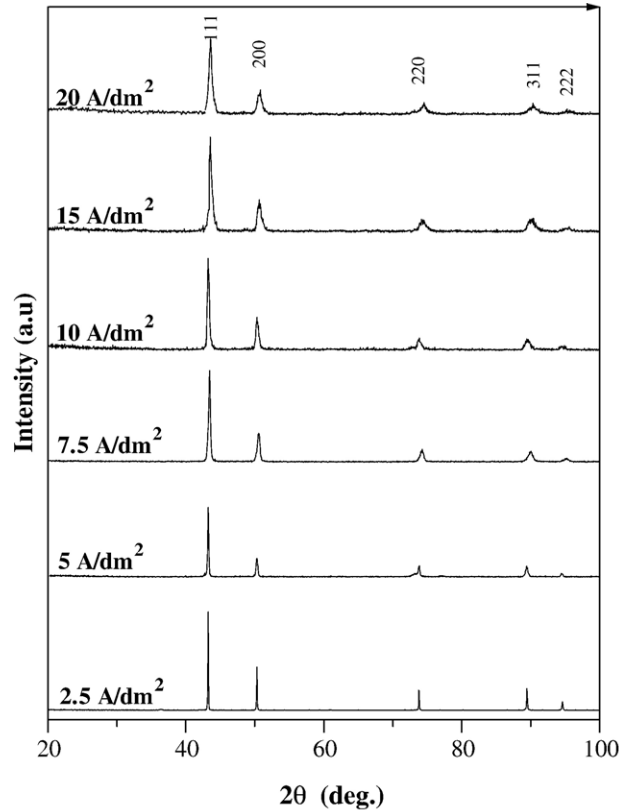

Fig. 5. X-ray diffraction pattern of the Cu–Ni alloy films obtained by PED at 2.5, 5, 7.5, 10, 15 and 20 A/dm^2 after subjecting them for vacuum annealing at 400 °C for 1 h.

The surface morphology of the Cu–Ni alloy films obtained at 2.5, 5.0, 7.5, 10, 15 and 20 A/dm^2 is depicted in Fig. 2(a) to (f), respectively. It is evident from Fig. 2(a)–(f) that the deposition is uniform throughout and the exhibits a cauliflower-like appearance [24]. The decrease in grain size with increase in current density is clearly evident. Energy dispersive X-ray (EDX) analysis reveals that the Cu–Ni alloy films have a stoichiometry of $Cu_{0.98}Ni_{0.02}$, $Cu_{0.95}Ni_{0.05}$, $Cu_{0.89}Ni_{0.11}$, $Cu_{0.77}Ni_{0.23}$, $Cu_{0.56}Ni_{0.44}$ and $Cu_{0.38}Ni_{0.62}$ that are obtained at 2.5, 5, 7.5, 10, 15 and 20 A/dm^2, respectively.

Fig. 3 shows the X-ray diffraction pattern of Cu–Ni alloy films obtained at 2.5–20 A/dm^2 in as-deposited condition. All the six films exhibit the presence of (111), (200) and (220) reflections indicating the f.c.c. structure of the Cu–Ni alloy (JCPDS file card no.: 07-1406). A shift is observed in the diffraction angle towards higher angles as the nickel content of the alloy film is increased. To substantiate this, the lattice constant (a) of the Cu–Ni alloy films is determined using the f.c. c. Cu–Ni diffraction angle and the Bragg's equation [25]. The lattice constant a is found to decrease with increase in the nickel content of the Cu–Ni alloy film (Fig. 4) in accordance with the Vegard's law [26]. Ghosh et al. [23] have also reported a decrease in the lattice constant of Cu–Ni alloy film with increase in nickel content of the film. The crystallite size of the Cu–Ni alloy films, determined using the Scherrer's formula [25,26] for the most intense (111) reflection, lies in the range of 15 to 46 nm and is found to be a function of the deposition current density; the higher the current density, the lower is the crystallite size (Table 2).

Fig. 5 shows the X-ray diffraction pattern of Cu–Ni alloy films obtained at 2.5–20 A/dm^2 after vacuum annealing at 400 °C for 1 h. Obviously, there is an increase in the intensities of (111), (200) and (220) reflections. Besides, the reflections from (311) and (222) planes, which are relatively weak in as-plated condition (Fig. 3), became quite evident after annealing. After annealing, a slight increase in the lattice constant of the Cu–Ni alloy films was observed. The crystallite size of

Table 2
Grain size, lattice constant and cell volume of PED nanocrystalline Cu–Ni alloy deposits both in as-plated and vacuum annealed (400 °C/1 h) conditions

Deposition current density (A/dm^2)	Cu–Ni alloy deposit	Grain size (nm)		Lattice parameter $a=b=c$ (Å)		Cell volume a^3 (Å^3)	
		As-plated	Vacuum annealed [a]	As-plated	Vacuum annealed [a]	As-plated	Vacuum annealed [a]
2.5	$Cu_{0.98}Ni_{0.02}$	46	114	3.623 (4)	3.626 (4)	47.572	47.690
5.0	$Cu_{0.95}Ni_{0.05}$	35	86	3.602 (8)	3.617 (0)	46.765	47.320
7.5	$Cu_{0.89}Ni_{0.11}$	28	54	3.597 (3)	3.611 (6)	46.551	47.108
10.0	$Cu_{0.77}Ni_{0.23}$	19	29	3.583 (2)	3.607 (3)	45.998	46.929
15.0	$Cu_{0.56}Ni_{0.44}$	17	25	3.562 (3)	3.600 (4)	45.194	46.656
20.0	$Cu_{0.38}Ni_{0.62}$	15	20	3.541 (4)	3.591 (1)	44.399	46.307

[a] At 400 °C for 1 h.

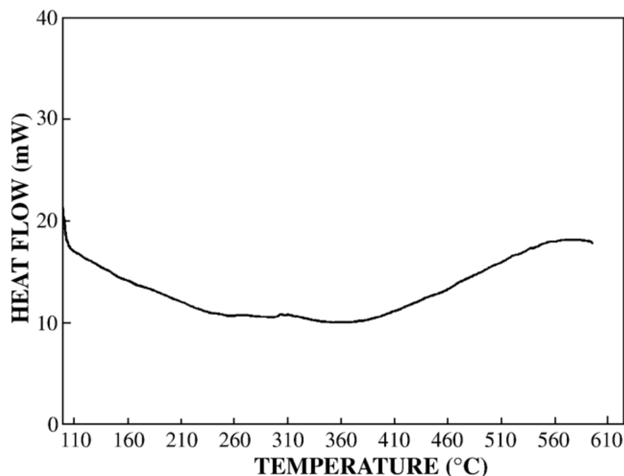

Fig. 6. DSC trace of PED $Cu_{0.89}Ni_{0.11}$ alloy film.

the Cu–Ni alloy films is increased from 20 to 114 nm, following annealing (Table 2).

Fig. 6 depicts the DSC trace of PED nanocrystalline $Cu_{0.89}Ni_{0.11}$ alloy film, in the temperature range of 100 to 550 °C. The DSC trace exhibits a single broad peak in the temperature range studied. In metallic films obtained by DC plating, an endothermic peak, due to the release of occluded hydrogen, normally occurs around 200 °C [27,28]. The absence of this endothermic peak in Fig. 6 indicates the absence of occluded hydrogen in the $Cu_{0.89}Ni_{0.11}$ alloy film obtained by PED process. The occurrence of a broad exothermic peak has been observed earlier for electrodeposited metallic alloys [28–32]. Zhou and Bakker [33] have also observed a similar broadening of the exothermic peak during the phase transformation of intermetallic compounds obtained by mechanical milling. The formation of a broad exothermic peak in DSC trace could be attributed to the (i) the relaxation of lattice defects, stresses and an increase in the short-range ordering; (ii) development of a long-range order; and (iii) crystallite growth from nanocrystalline state to microcrystalline state [33]. The lattice defects like screw dislocations and stacking faults are inevitable in electrodeposition processes [34]. It is expected that the process of ordering in the electrodeposited materials also takes place by a more or less similar mechanism.

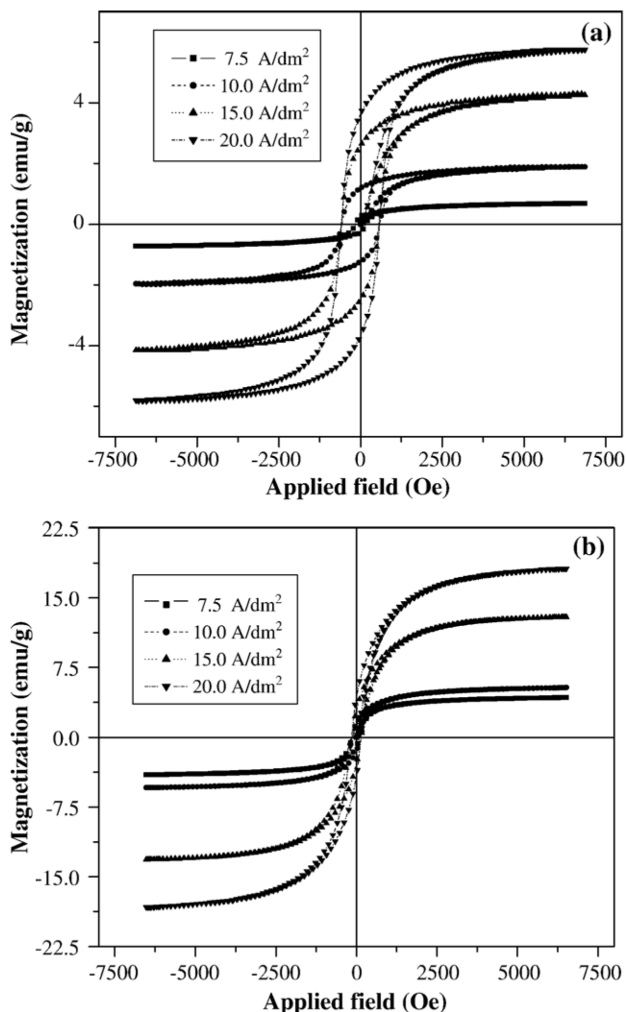

Fig. 7. Hysteresis loop of the Cu–Ni alloy films obtained by PED at 7.5, 10, 15 and 20 A/dm^2 (a) as-plated condition and (b) vacuum annealed at 400 °C for 1 h.

Table 3
Magnetic parameters of the PED nanocrystalline Cu–Ni alloy deposits

Deposition current density (A/dm^2)	Composition of the Cu–Ni alloy deposit	Remanence (M_r) (emu/g)	Magnetization (M_s) (emu/g)
As-plated condition			
7.5	$Cu_{0.89}Ni_{0.11}$	0.253	0.8942
10.0	$Cu_{0.77}Ni_{0.23}$	0.5432	2.009
15.0	$Cu_{0.56}Ni_{0.44}$	1.044	4.346
20.0	$Cu_{0.38}Ni_{0.62}$	1.609	5.868
Vacuum annealed at 400 °C for 1 h			
7.5	$Cu_{0.89}Ni_{0.11}$	1.071	4.231
10.0	$Cu_{0.77}Ni_{0.23}$	1.462	5.43
15.0	$Cu_{0.56}Ni_{0.44}$	2.875	13.09
20.0	$Cu_{0.38}Ni_{0.62}$	4.208	18.35

The VSM studies reveal that, among the six types of Cu–Ni alloy films of the present study, the films prepared at 2.5 and 5.0 A/dm^2 are diamagnetic, whereas those prepared using 7.5, 10, 15 and 20 A/dm^2 exhibit ferromagnetic activity. Since copper is diamagnetic [35] and nickel is ferromagnetic [36,37], it is obvious to expect the Cu–Ni alloy films, which are very rich in copper to exhibit diamagnetic character and vice versa. According to the Cu–Ni alloy phase diagram, the Cu–Ni alloy films obtained at 2.5–7.5 A/dm^2 fall under the category of diamagnetic [38]. The weak ferromagnetic activity exhibited by $Cu_{0.89}Ni_{0.11}$ alloy film obtained at 7.5 A/dm^2 may be due to the diffusion of nickel in copper matrix. Cu–Ni films prepared at 10, 15 and 20 A/dm^2 are found to be ferromagnetic and the ferromagnetic nature increases with increase in Ni content of the alloy film. Preparation of such alloy films with varying ferromagnetic activity has been a subject of long standing interest [39,40]. Fig. 7(a) shows the hysteresis loop of the Cu–Ni alloy films obtained at 7.5, 10, 15 and 20 A/dm^2 in the as-deposited condition. The saturation magnetization increases with the increase in nickel content of the Cu–Ni alloy films (Table 3). The dependence of saturation magnetization on the nickel content of the Cu–Ni alloy films has also been reported by Kubinski and Holloway [41]. Fig. 7(b) shows the hysteresis loop of the Cu–Ni alloy films after vacuum annealing at 400 °C for 1 h. It is evident that, after annealing, there is an increase in the saturation magnetization (Table 3), which is due to the atomic ordering in the f.c.c. structure. However, there is no direct evidence for order–disorder transition that has been found from XRD as the difference in scattering power of nickel and copper is too small.

4. Conclusion

From the study, it can be concluded that nanocrystalline Cu–Ni alloy films with uniformity and desirable characteristics could be prepared by pulsed electrodeposition process using sodium citrate-based plating bath. The film composition, lattice constant and magnetic properties of the films are functions of the applied current density and duty cycle. The Cu–Ni alloy films have a stoichiometry of $Cu_{0.98}Ni_{0.02}$, $Cu_{0.95}Ni_{0.05}$, $Cu_{0.89}Ni_{0.11}$, $Cu_{0.77}Ni_{0.23}$, $Cu_{0.56}Ni_{0.44}$ and $Cu_{0.38}Ni_{0.62}$ that are obtained at 2.5, 5, 7.5, 10, 15 and 20 A/dm^2, respectively, and they possess a f.c.c. structure. The lattice constant decreases with increase in the nickel content of the Cu–Ni alloy film. The crystallite size lies in the range of 15 to 46 nm for as-plated films and is a function of the applied current density, i.e., higher the current density, lower the crystallite size. Vacuum annealing at 400 °C for 1 h enables an increase in intensities of the (111), (200) and (220) planes, and also makes evident of the reflections from (311) and (222) planes. Annealing causes a slight increase in lattice constant of the Cu–Ni alloy film, whereas the crystallite size increased from 20 to 114 nm after annealing. VSM studies reveal that, among the six types of Cu–Ni alloy films, the films obtained at 2.5 and 5.0 A/dm^2 are diamagnetic, the one obtained at 7.5 A/dm^2 exhibits a weak ferromagnetic activity, whereas those obtained at 10, 15 and 20 A/dm^2 are ferromagnetic. The saturation magnetization increases with the increase in nickel content of the Cu–Ni alloy film.

Acknowledgement

The authors express their sincere thanks to Prof. P.R. Subramanian, Head, Department of Nuclear Physics, University of Madras, Chennai, for his constant support and encouragement to carry our this research work. This work is supported by UGC-SAP and DST-FIST programs of the Department of Nuclear Physics, University of Madras, Chennai.

References

[1] P.S. Peercy, Nature 406 (6799) (2000) 1023.
[2] C. Suryanarayana, C.C. Koch, Hyperfine Interact. 130 (1–4) (2000) 5.
[3] D. Kim, D.-Y. Park, B.Y. Yoo, P.T.A. Sumodjo, N.V. Myung, Electrochim. Acta 48 (7) (2003) 819.
[4] D.-Y. Park, N.V. Myung, M. Schwartz, K. Nobe, Electrochim. Acta 47 (18) (2002) 2893.
[5] M.S. Loffer, H. Natter, R. Hempelmann, K. Wippermann, Electrochim. Acta 48 (20–22) (2003) 3047.
[6] V.M. Dubin, IEEE Proceedings on Internet, Interconnect Technology Conference, vol. 1, 2001, p. 271.
[7] S.H. Kim, J.Y. Kim, J. Yu, T.Y. Lee, J. Electron. Mater. 33 (2004) 948.
[8] A. Benner, Electrodeposition of Alloys: Principle and Practices, vol. 1, Academic Press, New York, 1963.
[9] W.Z. Friend, Corrosion of Nickel and Nickel Alloys, 248, Wiley-Interscience, New York, 1980, p. 95.
[10] J.R. Ross, J.P. Celis, C. Buelens, D. Goris, Proc. Metall. 3 (1984) 177.
[11] I. Bakonyi, E. Toth-Kadar, J. Toth, T. Becsei, T. Tarnoczi, P. Kamasa, J. Phys., Condens. Matter 11 (1999) 963.
[12] B.H. Priscott, Trans. Inst. Met. Finish. 36 (1959) 93.
[13] H. Natter, T. Krajewski, R. Hempelmann, Ber. Bunsen-Ges. Phy. Chem. 100 (1996) 55.
[14] H. Natter, R. Hempelmann, J. Phys. Chem. 100 (1996) 19525.
[15] H. Natter, M. Schmelzer, R. Hempelmann, J. Mater. Res. 13 (5) (1998) 1186.
[16] I. Kazeminezhad, W. Schwarizacher, J. Magn. Magn. Mater. 226–230 (2003) 1630.
[17] J.C. Puippe, F. Leeman, Theory and Practice of Pulse Plating, American Electrodeplaters and Surface Finishers Society (AESF), Orlando, 1986.
[18] D. Landolt, Oberfl.-Surf. 1 (1984) 6.
[19] K. Vu Quang, E. Chassaing, B. Le Viet, J.P. Celis, J.R. Ross, Met. Finish. 83 (10) (1985) 25.
[20] R.Y. Ying, J. Electrochem. Soc. 135 (1988) 2957.
[21] L.H. Bennett, L.J. Swartzendruber, D.S. Lashmore, R. Oberle, Phys. Rev., B Condens. Matter 40 (7) (1989) 4633.
[22] L.H. Bennett, L.J. Swartzendruber, H. Ettedui, U. Atzmony, J. Appl. Phys. 67 (9) (1990) 4904.
[23] S.K. Ghosh, A.K. Grover, G.K. Dey, M.K. Totlani, Surf. Coat. Technol. 126 (2000) 48.
[24] L. Li, Y. Zhang, S. Deng, Y. Chen, Mater. Lett. 4363 (2003) 1.
[25] Michael M. Woolfson, An Introduction of X-ray Crystallography, 2nd editionCambridge University Press, 1997.
[26] B.D. Cullity, Element of X-ray Diffraction, 2nd edition, Addison-Wesley Publishing Company, Inc., 1988.
[27] R.A. Dunlap, K. Dini, J. Phys. F: Met. Phys. 14 (1994) 2797.
[28] A. Stephen, M.V. Ananth, V. Ravichandran, in: A.K. Singh (Ed.), Advanced X-ray Techniques in Research and Industry, Capital Publishing Company, New Delhi, 2006, pp. 485–491.
[29] G.H. Zhou, M.J. Zwanenburg, H. Bakker, J. Appl. Phys. 78 (1995) 3438.
[30] M.H. Bara, S. Surinach, J. Malagelada, M.T. Clavaguera, S. Gialanella, R.W. Chan, Acta Mater. 41 (1993) 1065.
[31] A.R. Yavari, P. Crespo, E. Pulido, A. Hernando, G. Fillion, P. Leihuillerir, M.D. Baro, S. Surinach, in: A.R. Yavari (Ed.), Ordering and Disordering in Alloys, Applied Science, London, 1992, p. 65.
[32] U. Klement, U. Erb, K.T. Aust, Nanostruct. Mater. 6 (1995) 581.
[33] G.H. Zhou, H. Bakker, Phys. Rev., B Condens. Matter 49 (1994) 12507.
[34] R.W. Hiton, L.H. Schwartz, J.B. Chochen, J. Electrochem. Soc. 110 (1963) 103.
[35] D. Jiles, Introduction to Magnetism and Magnetic Materials, 1st edition, Chapman Hall, London, 1991.
[36] B.D. Cullity, Introduction to Magnetic Materials, Addison, Wesley Reading, MA, 1972.
[37] R.C. Handley, Modern Magnetic Materials, Wiley, New York, 2000.
[38] Phil. Max Hansen, Kurt Anderko, Constitution of Binary Alloys, 2nd edition, Mc Graw-Hill Book company, New York, 1958, p. 601.
[39] P.A. Stampe, G. Willams, J. Phys., Condens. Matter 10 (1998) 6771.
[40] G.S. Brady, H.R. Clauser, J.A. Vaccori, Materials Handbook, 15th editionMc Graw-Hill Professional, 2002.
[41] D.J. Kubinski, H. Holloway, J. Appl. Phys. 77 (6) (1995) 2508.